

Journal Pre-proof

Discovery of novel allosteric site and covalent inhibitors of FBPase with potent hypoglycemic effects

Yunyuan Huang, Lin Wei, Xinya Han, Haifeng Chen, Yanliang Ren, Yanhong Xu, Rongrong Song, Li Rao, Chen Su, Chao Peng, Lingling Feng, Jian Wan



PII: S0223-5234(19)30901-8

DOI: <https://doi.org/10.1016/j.ejmech.2019.111749>

Reference: EJMECH 111749

To appear in: *European Journal of Medicinal Chemistry*

Received Date: 25 May 2019

Revised Date: 20 September 2019

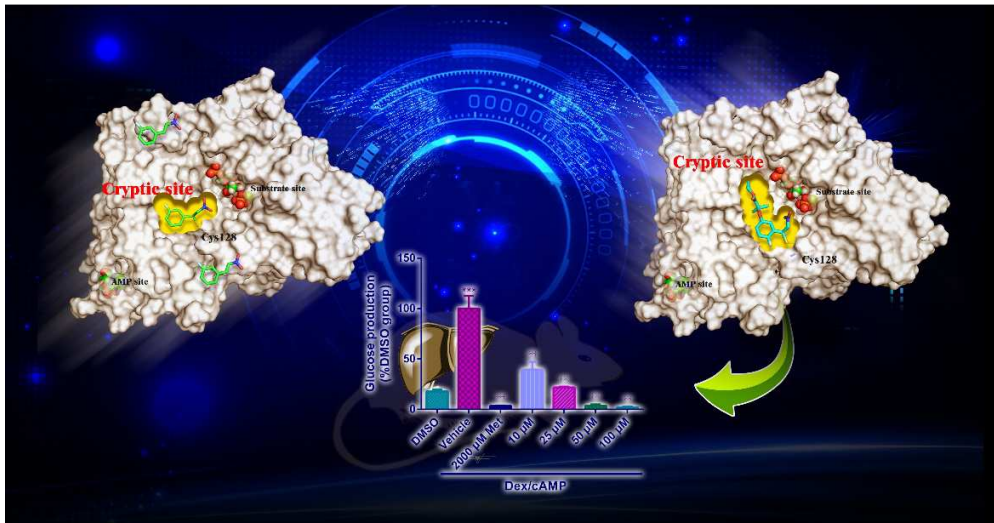
Accepted Date: 28 September 2019

Please cite this article as: Y. Huang, L. Wei, X. Han, H. Chen, Y. Ren, Y. Xu, R. Song, L. Rao, C. Su, C. Peng, L. Feng, J. Wan, Discovery of novel allosteric site and covalent inhibitors of FBPase with potent hypoglycemic effects, *European Journal of Medicinal Chemistry* (2019), doi: <https://doi.org/10.1016/j.ejmech.2019.111749>.

This is a PDF file of an article that has undergone enhancements after acceptance, such as the addition of a cover page and metadata, and formatting for readability, but it is not yet the definitive version of record. This version will undergo additional copyediting, typesetting and review before it is published in its final form, but we are providing this version to give early visibility of the article. Please note that, during the production process, errors may be discovered which could affect the content, and all legal disclaimers that apply to the journal pertain.

© 2019 Published by Elsevier Masson SAS.

Graphical Abstract.



Discovery of novel allosteric site and covalent inhibitors of FBPase with potent hypoglycemic effects

Yunyuan Huang,^{1,#} Lin Wei,^{1,#} Xinya Han,^{1,2,#} Haifeng Chen,^{1,3,#} Yanliang Ren,^{1,} Yanhong Xu,¹ Rongrong Song,¹ Li Rao,¹ Chen Su,⁴ Chao Peng⁴, Lingling Feng,¹ Jian Wan,^{1,*}*

¹International Cooperation Base of Pesticide and Green Synthesis (Hubei), Key Laboratory of Pesticide & Chemical Biology (CCNU), Ministry of Education, Department of Chemistry, Central China Normal University, Wuhan 430079, China

²School of Chemistry and Chemical Engineering, Anhui University of Technology, Maanshan 243002, China

³Ocean College, Beibu Gulf University, Qinzhou 535011, Guangxi, P. R. China

⁴ National Facility for Protein Science in Shanghai, Zhangjiang Lab, Shanghai, 201210, China

Highlights

- A new cryptic allosteric site (C128) in FBPase was discovered.
- Several nitrostyrene compounds (**12** and **13**) exhibiting potent FBPase inhibitions were found covalently bind to C128 site on FBPase.
- The N125-S124-S123 pathway was involved in allosteric signaling transmission between C128 and active site.
- The treatments of compounds **14a**, **14c**, **14i** or **14n** led to potent inhibition of glucose production, as well as decreased triglyceride and total cholesterol levels in mouse primary hepatocytes.

KEYWORDS Fructose-1,6-bisphosphatase (FBPase), Novel allosteric site, Covalent inhibitors, Fragment-based drug design

Abstract

Fructose-1,6-bisphosphatase (FBPase) is an essential enzyme of GNG pathway. Significant advances demonstrate the FBPase plays a critical role in treatment of diabetes. Numerous FBPase inhibitors were developed by targeting AMP site, nevertheless, none of these inhibitors has exhibited suitable potency and druggability. Herein, a new allosteric site (C128) on FBPase was discovered, and several nitrostyrene compounds exhibiting potent FBPase inhibitions were found covalently bind to C128 site on FBPase. Mutagenesis suggest that C128 is the only cysteine that can influence FBPase inhibition, the N125-S124-S123 pathway was most likely involved in allosteric signaling transmission between C128 and active site. However, these nitrostyrenes may bind with multiple cysteine besides C128 in FBPase. To improve pocket selectivity, a series of novel compounds (**14a-14n**) were re-designed rationally by integrating fragment-based covalent virtual screening and machine-learning-based synthetic complexity evaluation. As expected, the mass spectrometry validated that the proportion of title compounds binding to the C128 in FBPase was significantly higher than that of nitrostyrenes. Notably, under physiological and pathological conditions, the treatment of compounds **14b**, **14c**, **14i** or **14n** led to potent inhibition of glucose production, as well as decreased triglyceride and total cholesterol levels in mouse primary hepatocytes. We highlight a novel paradigm that molecular targeting C128 site on FBPase can have potent hypoglycemic effect.

1. Introduction

Fructose-1,6-bisphosphatase (FBPase) is an essential enzyme of the gluconeogenesis (GNG) pathway, and a predominant factor involved with increased hepatic glucose output[1, 2]. Numerous FBPase inhibitors have been explored as potential agent for the treatment of diabetes, especially type 2 diabetes mellitus (T2D),[3, 4] thus FBPase also represents an attractive target for diabetes treatment.[5-9] To the best of our knowledge, most FBPase inhibitors reported previously[10] bind to the AMP site on FBPase via non-covalent interactions (e.g., hydrogen-bonds, salt bridges, *van der Waals* interactions). Nevertheless, none of these inhibitors exhibit suitable potency, specificity or biological activity, except compound **MB06322(CS-917)**,[11, 12] Although **MB06322** has been undergoing clinical evaluation,[13, 14] phase I clinical studies have indicated that **MB06322** can cause lactic acidosis in human hepatocytes[15].

On the other hand, covalent drugs have been profoundly successful in the treatment of a wide array of human diseases. In particular, the clinical success of **ibrutinib**[16] and **afatinib**[17] has prompted a resurgence of interest in covalent inhibitor discovery.[18, 19] Compared with traditional non-covalent drugs, covalent inhibitors possess exceptionally high potency, ligand efficiency and exhibit long-lasting effects, because covalent bonds are significantly stronger than non-covalent interactions.[20, 21] In fact, previous covalent drugs are usually designed by attaching a “covalent warhead” to non-covalent inhibitors. For instance,

the covalent drug **afatinib**, targeting a Bruton's tyrosine kinase-associated cysteine for treatment of non-small-cell lung carcinomas (NSCLCs), stem from the non-covalent inhibitor **gefitinib** and an acrylamide "warhead"[22, 23]. In other words, the non-catalytic residues that might covalently react with the "warhead" are indispensable[20, 24] for the discovery of covalent inhibitors. As an uncommon residue, non-catalytic cysteine is not highly conserved in the enzyme sequence[23, 25] and is often observed in the binding pocket of covalent inhibitors[20, 26] due to the electrostatic properties of residues. Targeting of non-catalytic cysteine residues has emerged as an indispensable strategy for the design of drugs and inhibitors against protein kinases[22, 27], such as G-protein-coupled receptors (GPCRs)[28], proteases[29] and GTPases[30]. Many covalent inhibitors that bind to non-catalytic cysteines of kinases, e.g., **ibrutinib**, **acalabrutinib**, **afatinib** and **osimertinib**, have been approved for commercial use by US FDA[20].

Inspired by the deficiency of traditional FBPase inhibitors[15] and the benefit of covalent drugs[16] [17], our approach reported here will focus on the exploration of novel cryptic allosteric site and covalent inhibitors of FBPase. Herein, a cryptic site (cysteine 128) on FBPase was identified and verified using an electrophilic fragment-based screen strategy[31, 32] for the first time. Furthermore, nitrostyrene derivatives that covalently bind to the C128 site of FBPase *via* a nitrovinyl covalent warhead, which is also included in **ranitidine**,[33, 34] were screened in this work. However, the Mass Spectrometry (MS) showed that nitrostyrene might bind with more than one cysteine residue besides C128 in FBPase. To improve the pocket

selectivity, a drug moiety was attached to nitrostyrene for the generation of new compounds by integrating the fragment-based covalent virtual screening (FBCVS) protocol and machine-learning-based synthetic complexity evaluation based on the C128 site of FBPase. In addition, T2D has become a prevalent public health concern around the world, and is associated with other cardiovascular complications, such as hypertension[35], hyperlipidemia[36, 37], and atherosclerosis[38]. Diabetes mellitus is associated with an increased risk of dyslipidemia and coronary artery disease. Patients with T2D increased the incidence of coronary artery disease and dyslipidemia that is 2- to 6-fold compared to persons without diabetes, and this epidemic has remained unabated in recent years.[36][39] Therefore, the strategy of attaching a fragment with anti-dyslipidemic function to nitrostyrene may contribute to improve the selectivity and dual-functionalization of resulting compounds. As expected, the proportion of title compounds covalently bound to the C128 site of FBPase increased significantly compared with that of nitrostyrene. The enzymatic experiments indicated that compound **14b** exhibited the potential inhibitory activity against FBPase with an IC_{50} of 0.61 μ M. Importantly, compounds **14b**, **14c**, **14i** or **14n** showed excellent inhibition of glucose production, as well as the ability to decrease triglycerides (TG) and total cholesterol (TC) levels.[40]

2. Results and discussions

2.1 Screening of covalent warheads.

Cysteine-reactive screening is the most popular strategy for discovery of cryptic site. For instance, the C290 site of caspase-7 was identified by using the library

compound **FICA**[41]. Discovery of the KRAS^{G12C} allosteric site also benefited from this screening method[42]. According to crystal structure (PDB ID: 1FTA), there were seven cysteines (Fig. S1) near the substrate (FBP) or AMP binding pocket[43] on FBPase, but no remarkable interaction between these cysteines and the substrate FBP/AMP[44] could be observed. To our knowledge, cysteine reacts easily with reactive electrophilic species[45]. Therefore, reactive electrophilic species that are commonly present in covalent drugs[46] or endogenous species, were selected as probes to identify a suitable covalent warhead that reacted with the cysteine in FBPase. As shown in Fig. S2, compound **10** (9-nitro-oleic acid) exhibited higher FBPase inhibition ($IC_{50} = 58 \mu\text{M}$) than the other compounds (**1–9**). In fact, the lipid containing nitrovinyl moiety is involved in some post-translational modification of proteins *in vivo*[47-49]. Ranitidine[33, 34] is also a well-known drug with a nitrovinyl group. **Dimethyl fumarate** (**2**), derived from the endogenous electrophilic species **6** (fumarate)[50], is used for the treatment of multiple sclerosis. These evidences suggest that nitrovinyl (**10**) moiety is most likely a suitable covalent warhead for reaction with the cysteine in FBPase.

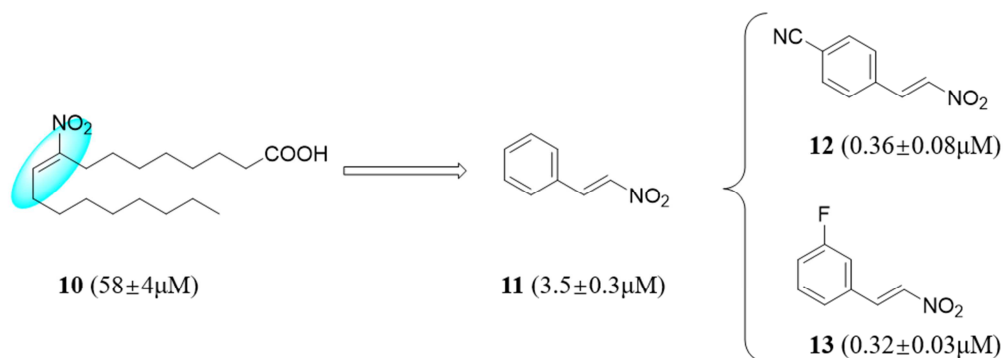


Fig. 1. The endogenous **nitrostyrene** electrophilic **10** (9-nitro-oleic acid) and its

derivatives (**11**, **12** and **13**) structure, as well as their inhibition activities against FBPase.

2.2 Covalent binding of nitrostyrene to multiple cysteines in FBPase.

Although compound **10** could inhibit FBPase, it is difficult to further synthesize and optimize because its structure is too complex. To identify the binding pocket of nitrovinyl covalent warhead on FBPase, three simple nitrovinyl derivatives (**11**, **12** and **13**) were further synthesized. Fig. 1 shows that cyano- and fluorine-substituted nitrostyrene (**12** and **13**) exhibited a 150-fold increase in inhibitory activities compared with compound **10** ($IC_{50} = 58 \mu M$). To verify that these nitrostyrene derivatives may react with the thiol group, 100 μM compound **12** was further reacted with β -mercaptoethanol (β ME). The UV-visible absorption (Fig. S3A) gradually decreased as the β ME concentration increased, this suggests that compound **12** can actually react with the thiol group. The K_d (54 μM) was determined by plotting the proportion of the β ME adduct vs β ME concentration (Fig. S3B). In fact, nitrovinyl has also been shown to be highly biologically active[51, 52] *via* reactions with the thiol group of cysteine. For instance, **dipeptidyl nitroalkene** might covalently bind to the CYS25 of the proteases rhodesain and cruzain via the nitrovinyl moiety[53]. 3,4-Methylenedioxy- β -nitrostyrene has been demonstrated to inhibit NLRP3 ATPase activity by covalently binding to the cysteine of NLRP3 for the therapy inflammasome[54].

To determine the number of cysteine residues in FBPase that could react with nitrostyrene, compounds **12** and **13** were incubated with FBPase for 2 h. Then, the

covalent adducts were detected by Liquid chromatography–mass spectrometry (LC–MS)[55]. The MS results (Fig. S4) showed that more than two nitrostyrene derivatives (**12** and **13**) could covalently bind with FBPase.

2.3 Identifying the cryptic allosteric site (C128) on FBPase.

To improve the pocket selectivity of nitrostyrene, we first identified a functional cysteine pocket that can regulate the catalytic activities of FBPase. For this purpose, seven cysteines in FBPase were mutated to serine. Table 1 shows that only the C128S mutation could result in significant decrease in the inhibitory activity of **12** and **13** ($IC_{50} > 350 \mu M$), decreasing the FBPase activity by more than 1000-fold compared with the activity of wild-type (WT) FBPase. This evidence suggests that C128 is the only cysteine that can influence FBPase inhibition by **12** and **13**, although both compounds may covalently bind with three cysteine residues on FBPase.

Table 1. Kinetic parameters of seven cysteine mutations of FBPase, and the IC_{50} of **12** / **13** against mutations and WT.

	WT	C38S	C92S	C116S	C128S	C179S	C183S	C281S
V_{max} (U/mg)	4.0±0.2	1.3±0.1	1.6±0.1	1.6±0.2	2.7±0.2	2.3±0.1	3.8±0.2	3.6±0.1
k_{cat} (1/s)	2.5±0.1	0.79±0.04	0.99±0.07	1.0±0.1	1.7±0.1	1.4±0.1	2.4±0.2	2.2±0.1
K_m (mM)	0.020±0.002	0.043±0.005	0.051±0.009	0.093±0.009	0.10±0.02	0.083±0.006	0.12 ± 0.02	0.12±0.01
K_a (mM)	0.14±0.02	0.50±0.06	0.11±0.01	0.13±0.01	1.1±0.1	0.11±0.01	0.16±0.02	0.23±0.02
AMP IC_{50} (μM)	2.3±0.1	0.37±0.02	1.3±0.2	0.82±0.05	5.2±1.2	1.0±0.1	6.3±1.0	1.1±0.1
12 IC_{50} (μM)	0.36±0.08	0.49±0.08	0.34±0.02	0.33±0.04	> 350	0.43±0.06	0.44±0.02	0.61±0.03
12 (IC_{50}^M / IC_{50}^W)	1	1.4	0.97	0.94	> 1000	1.2	1.2	1.7
13 IC_{50} (μM)	0.32±0.03	1.2±0.3	0.62±0.10	1.1±0.2	>350	0.89±0.10	0.92±0.21	2.3±0.2
13 (IC_{50}^M / IC_{50}^W)	1	3.8	1.9	3.4	> 1010	2.8	2.8	7.2

The crystal structure of FBPase (*R* state, PDB ID: 1EYI) shows that C128 is located on the interface of two subunits, and is distant (12 Å) from the substrate

catlysis site (Fig. S5); thus, direct interaction of C128 and the catalytic site of FBPase is difficult to achieve. In order to verify the allosteric regulation mechanism of C128, the possible binding model of FBPase and compound **12** was predicted using Autodock 4[56] and the molecular dynamic (MD) simulation was performed. To our knowledge, there are two famous mechanisms to explain the reaction of cysteine and nitroethylene warheads: One was slow-binding mechanism[57] that sulfur group of cysteine attack the nitro group of nitroethylene warhead. The other was Michael addition mechanism [54, 58, 59] that nitroethylene warheads was recognized as Michael acceptor and undergo conjugate addition with thiol group. Hence, two possible binding modes (Michael acceptor or reaction between thiolate and nitro group) of nitrostyrene compounds and C128 of FBPase were used for the further simulations. As shown in Fig. 2A, the MD conformation of N125-S124-S123 (white) on FBPase almost overlaps with the crystal structure (PDB: 1EYI, green). However, if nitrostyrene acts as the Michael acceptor, C₇ of **12** was attacked by the C128 thiolate. The MD of FBPase+**12** (Fig. 2B, purple) result in the remarkable conformation change of N125-S124-S123 compared with that of Apo-FBPase (Fig. 2A, white). The nitro group of **12** and -CONH₂ group of N125 would repel each other, which cause the movement of N125 away from C128, in turn result in the movement (2.3 Å) of the S123 far from the phosphate of FBP. Similarly, if the reaction occurring between C128 thiolate and nitro group of **12**, the MD result (Fig. 2C) of FBPase+**12** (N₉ of **12** was attacked) also shows the remarkable conformation change of N125-S124-S123, and the movement of the S123 far from the phosphate of FBP (Fig. 2C, blue)

compared with that of Apo-FBPase (Fig. 2A, white). On the other hand, one hydrogen bond between S123 and the phosphate of FBP was observed in the crystal FBPase structure (Fig. S5). Thus, the addition of nitrostyrene **12** onto C128 could actually weaken the hydrogen-bond of S123--FBP (Fig. 2B and Fig. 2C) and inhibit FBPase catalysis activity through N125-S124-S123 allosteric signaling pathway, N125 is a most important residue on this pathway. Notably, our simulated results indicate that both covalent binding modes result in the same allosteric regulation mechanism of C128. Additionally, the addition of nitrostyrene **12** onto C128 could also result in the movement of Mg^{2+} (Fig. 2B) far from the phosphate of FBP about 2.5 Å. This result partly demonstrated that compound **12** may weaken the binding abilities of Mg^{2+} .

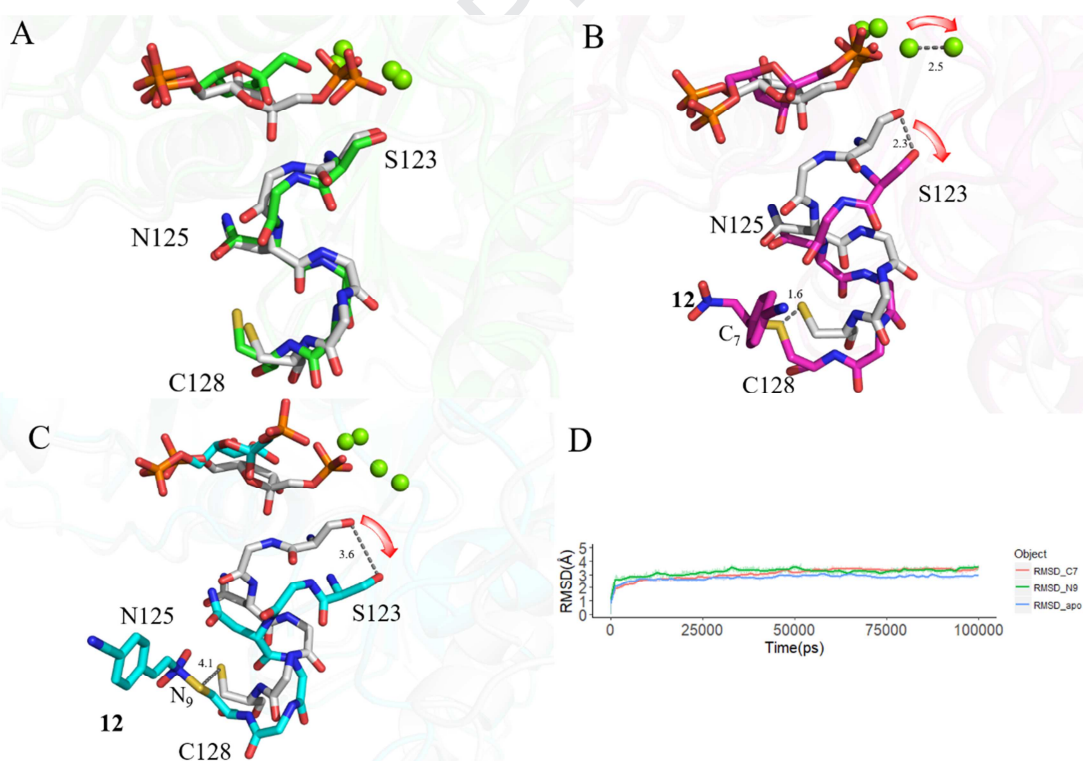


Fig. 2. Proposed conformation of compound **12** covalent binding to C128 simulated by molecular dynamic (MD). (A) Crystal FBPase structure (PDB:1EYI) was superposed with that (FBPase, white) of MD simulation, (B) The MD structures

superposition of Apo-FBPase (white) and FBPase+**12** (purple), with the binding model that the C₇ of **12** was attacked. (C) The MD structures superposition of Apo-FBPase (white) and FBPase+**12** (blue), with the binding model that N₉ of **12** was attacked. (D) Plots of the MD simulation root-mean-square deviation (RMSD, in Å) MD simulation vs time of FBPase and FBPase+**12**.

To verify the importance of this helix H4 pathway, the residues surrounding this network were further mutated to Ala. As listed in Table S1, the effects of D127A, R243A, R254A and Y258A mutations on the K_a (Mg²⁺ binding affinity) and IC₅₀ (**12** and **13**) values were almost negligible. According to the crystal structure of R state FBPase (Fig. S5) and the discussions mentioned-above, N125 is the residue (in helix 4) closest to C128 (3.3 Å), thus the addition of nitrostyrene (**12** or **13**) onto C128 will cause the remarkable movement of N125 away from C128, which in turn significantly decrease the FBPase activity. However, when N125 was mutated to Ala, N125-S124-S123 will move close to C128, which in turn result in the increase of FBPase activity. As expected, the N125A lead to more than 500-fold IC₅₀ increase (Table S1) of compounds **12/13** compared with WT (0.36 μM). In comparison, S124 is far from the C128 (6.8 Å), S124A could not remarkably affect the movement of N125-S124-S123. Correspondingly, S124A caused 3.8- and 37.8- fold increase of the IC₅₀ of compounds **12/13**. Furthermore, as shown in Table S1, the K_{cat} value of S123A (0.041 s⁻¹) decreased approximately 61-fold compared to that of the WT (2.5 s⁻¹), and S123A lacked detectable activity. This suggests that S123 is critical for the catalytic activity of FBP. These mutant results further confirm our speculation that

C128 could affect the catalytic activity of FBPase *via* H4 allosteric signaling pathway (N125-S124-S123), and N125 is a most important residue on H4 pathway.

Furthermore, the effect of Mg^{2+} on the inhibitory activities of **12** and **13** was also investigated. As illustrated in Fig. S6, at a fixed Mg^{2+} concentration, the relative activity of FBPase may gradually decrease with increasing concentration of compound **12** or **13**, however, the FBPase activities may increase as Mg^{2+} concentrations increase from 1 mM to 10 mM. This evidence suggests that both **12** and **13** may weaken the binding abilities of Mg^{2+} via the N125-S124-S123 pathway, thus competitively inhibiting Mg^{2+} .

Furthermore, $10\times$ the IC_{50} concentration of compounds **12** and **13** (Fig. S7) were incubated with FBPase for complete inhibition. Then, the mixture was diluted 20 folds and then detected enzyme catalysis activity. These assays reveal that compounds **12** and **13** covalently likely binds FBPase in a reversible manner. As documented previously, whether the reaction of nitroethylene warhead and target protein is slow-binding mechanism[57] or Michael addition mechanism[57, 60, 61], the corresponding reaction show reversible behavior. Thus, we believe that compound **12** most likely react with C128 of FBPase in a reversible behavior.

Taken together, these findings suggest that, in addition to the FBP and AMP sites, the C128 pocket of FBPase is a new non-catalytic site, which was identified by our group for the first time, and could be used for the discovery of novel covalent inhibitors against FBPase. Based on the document by Beglov et al.[32], such a binding site is not easily detectable, and is thus called a “cryptic site”.

2.4 Redesign of nitrostyrene-based covalent inhibitors (**14a-14n**).

Based on the MS experiments in Fig. S4, nitrostyrene could bind with more than one cysteine residue in FBPase, likely because nitrostyrene is very small, and can easily bind to multiple cysteine pockets. To improve the selectivity of these nitrostyrenes, rational optimization by attachment of drug moieties to nitrostyrene based on the cryptic allosteric pocket (C128) of FBPase is necessary. To achieve this purpose, a new FBCVS protocol (Fig. S8) based on the C128 pocket of FBPase was used to generate new hits. In fact, fragment-based approach[23] has been successfully used for identification of covalent inhibitors for RAS G12C from a library of disulfides, followed by conversion to an irreversible warhead.[62] Kathman et al. utilized a fragment-based screening method to test the ability to inhibit papain, a model cysteine protease.[63] The fragment-based approach has also been validated by a large number of fragment-to-lead studies reported in recent literature,[64] as well as by successful translation of more than 30 compounds to clinical studies, and by the introduction of two FDA approved drugs (**vemurafenib** and **venetoclax**) into the market. Nonetheless, fragment-based covalent inhibitors screening is rare. Moreover, ensuring the synthetic tractability of the resulting molecule generated by the FBCVS protocol remains challenging.[65] To overcome this challenge, the synthetic complexity score (SCscore) developed by Green et al.[66] and learned from Reaxys reaction database was used to evaluate the compounds designed by this FBCVS protocol for the first time.

In addition, patients with T2D increased the incidence of coronary artery disease and dyslipidemia that is 2- to 6-fold compared to persons without diabetes, and this epidemic has remained unabated in recent years.[36]:[39] Attaching a fragment with anti-dyslipidemic function to nitrostyrene may contribute to improvement of the selectivity of the resulting compounds, as well as to dual-functionalization of these compounds. Currently available anti-dyslipidemic drugs mainly include statins,[67, 68] fibrates,[69, 70] niacin[71] and ezetimibe[72], thus, functional moieties on these drugs were selected as fragment parameters (Fig. S9).

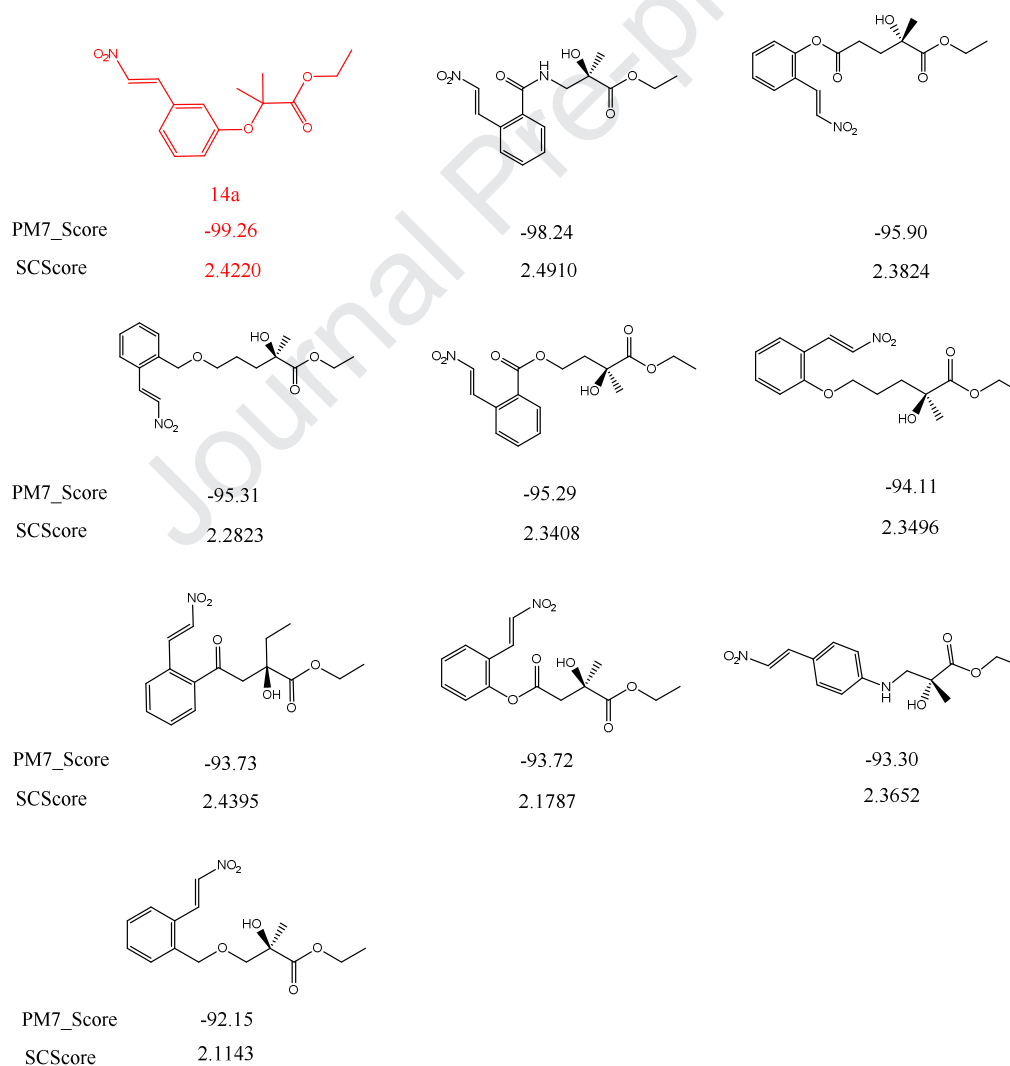
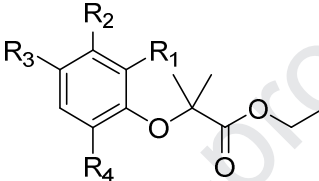


Fig. 3. Designed nitrostyrene derivatives (Top 10) by using FBCVS protocol; PM7_score is the binding energy calculated by PM7@MOPAC; SCScore is the

synthetic complexity score developed by Green[66] et al.

Combining PM7@MOPAC score and machine-learning-based synthetic complexity evaluation (ScScore), a second generation of nitrostyrene-based covalent inhibitors (**14a**, Table S2 and Fig. 3), which were *de novo* designed based on the cryptic allosteric site (C128) on FBPase.

Table 2. The inhibitory activities of synthesized compounds (**14a-14n**) against FBPase *in vitro*



Comps	R_1	R_2	R_3	R_4	IC ₅₀ (μM)
14a	H	Nitrovinyl	H	H	1.0±0.1
14b	H	Nitrovinyl	F	H	0.61±0.11
14c	H	Nitrovinyl	Cl	H	2.9±0.2
14d	H	Nitrovinyl	Br	H	0.79±0.12
14e	H	Nitrovinyl	H	Cl	0.83±0.14
14f	H	Nitrovinyl	H	OCHF ₂	1.6±0.2
14g	Nitrovinyl	H	H	H	2.7±0.1
14h	Nitrovinyl	H	F	H	7.0±0.3
14i	Nitrovinyl	H	Cl	H	8.2±0.3
14j	H	H	Nitrovinyl	H	3.1±0.4
14k	Cl	H	Nitrovinyl	H	1.6±0.3
14l	H	Cl	Nitrovinyl	H	1.8±0.2
14m	H	CH ₃	Nitrovinyl	H	5.4±0.5
14n	H	2Br-2-Nitrovinyl	Cl	H	0.84±0.07
AMP	-	-	-	-	2.3±0.1

FBPase inhibition by synthesized compounds. Although the anti-dyslipidemic fragment of clofibrate was attached to compound **11**, the inhibitory activities of **14a** compounds may be retained at approximately 1.0 μM (Table 2) compared with that of our previous nitrostyrene compound **11** (3.5 μM). To discover potent hit compounds, a

series of nitrostyrene derivatives were further synthesized (Table 2) and characterized (Supplementary Methods) to explore the structure-activity relationships (SARs). When a nitrovinyl group was introduced at R_2 of these compounds, the IC_{50} values of compounds **14a-14f** were 0.61~2.9 μM . When the R_1 position was replaced with a nitrovinyl group, the inhibitory activities of the title compounds (**14g-14i**) were decreased slightly, with IC_{50} values of 2.7~8.2 μM . In comparison, compounds with nitrovinyl substituents at the R_3 position (**14j-14m**) had IC_{50} values of 1.6-5.4 μM . To determine whether these compounds could also bind to the C128 site, we exploited compound **14b** as a probe molecule to explore the binding mode. As shown in Table S3, only the C128S mutations could remarkably affect the IC_{50} value of **14b**, causing an 820-fold increase compared to the wild type. These consequences demonstrated that C128 is extremely essential for the binding of **14b** and FBPase, and a covalent reaction likely occurs between **14b** and C128, similar to that observed for compound **11**.

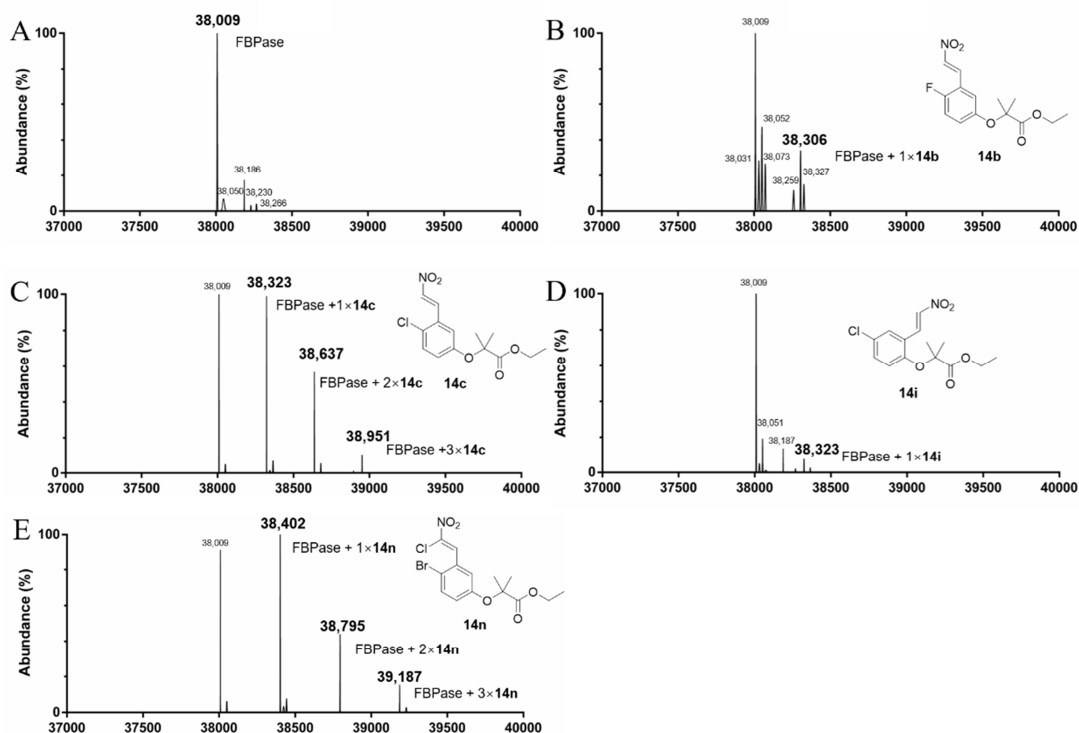


Fig. 4. Mass spectrometry of covalent binding of FBPase (A) and compounds, (B)FBPase+**14b**, (C) FBPase+**14c**, (D)FBPase+**14i**, (E) FBPase+**14n**

To further determine the number of cysteines in FBPase that may react with these compounds, MS analysis of FBPase+compound was also performed (Fig. 4). Fig. 4B shows that the main peak (38,009 Da) belongs to FBPase, and the peak at 38,306 Da belongs to FBPase+**14b**. These results suggest that **14b** might covalently bind with one cysteine on FBPase. Combining previous mutation experiments (Table S3) and this result (Fig. 4B), one could infer that **14b** predominately bind with C128 in FBPase. Similar to **14b**, **14i** could also specifically bind with C128 on FBPase as illustrated in Fig. 4D. Additionally, the mass spectra of FBPase and **14c** were also determined in Fig. 4C. Fig.4C clearly shows that, although the covalent interactions FBPase+2×**14c** and FBPase+3×**14c** occurred (based on the peaks at 38,637 Da and 38,951 Da), the predominant component was FBPase+**14c** (38,323 Da). Similar to **14c**,

14n could also bind to FBPase with three forms as illustrated in Fig. 4E

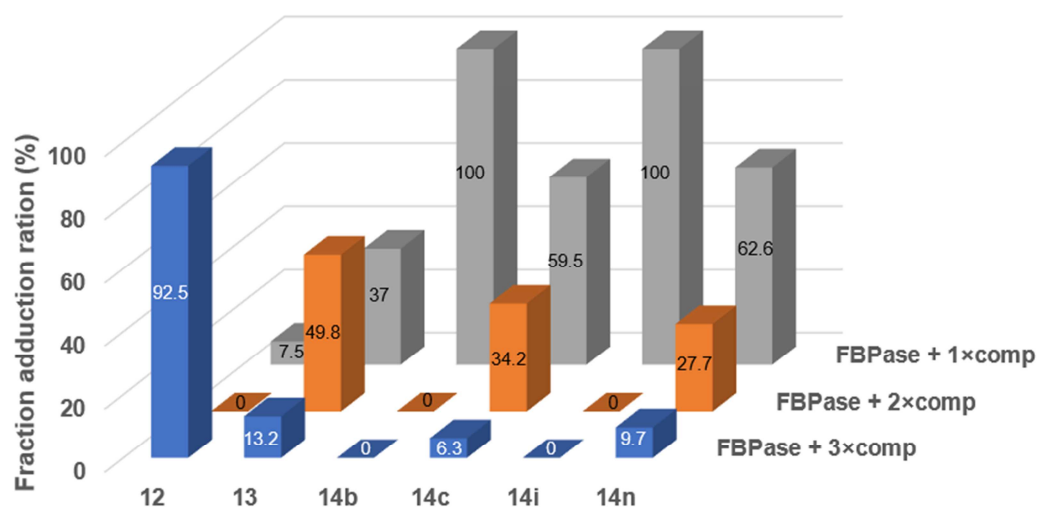


Fig. 5. The fraction adduction ratio of compounds (**12**, **13**, **14b**, **14c**, **14i** and **14n**) and FBPase complex (FBPase +1×comp, FBPase +2×comp, FBPase +3×comp).

In conclusion, the proportion (Fig. 5) of title compounds (**14a**, **14c**, **14i** or **14n**) that bound to the C128 site on FBPase increased compared with that of compounds **12/13**. These positive results indicate that anti-dyslipidemic fragments are predominantly accommodated in the C128 pocket of FBPase. The optimization strategy adopted in this study could remarkably improve the pocket selectivity of FBPase inhibitors.

2.5 Binding model of compound **14b** and FBPase.

As shown in Fig. S10A and Fig. S10B, the possible binding model for FBPase and **14b** act as Michael acceptor (C₇ of **14b** was attacked) was predicted using Autodock 4[56]. In Fig. S10A, the -NH₂ of R243 can form two hydrogen bonds with -NO₂ and -C=O of **14b**. The NH₂ moiety of R254 can form hydrogen bonds with -NO₂ of **14b**. Two hydrogen-bonds between S124 and **14b** could also be observed in Fig. S10A. In addition, another possible binding model for FBPase and **14b** (N₉ of

14b was attacked) was also predicted in Fig. S10C and Fig. S10D. As illustrated in Fig. S10C, the -OH group of S124 can form hydrogen bond with ether oxygen group of **14b**. A π - π staking interaction between the R243 and **14b** could be observed in Fig. S10C. The NH₂ moiety of R254 likely forms halogen bond with F of **14b**. To verify these binding modes, mutations of the critical residues mentioned-above were performed (Table S3). The IC₅₀ values of R243A (17 μ M) and R254A (12 μ M) increased 28- and 20-fold compared with that of WT FBPase (0.61 μ M). In addition, S124A result in 39-fold IC₅₀ increase of compounds **14b** compared with that of WT (0.61 μ M). These mutant results demonstrate the importance of residues S124, R254 and R243 for both binding modes of **14b** and FBPase. In addition, a weakly π - π interaction (3.6 Å) between benzene (Y258) and benzene (**14b**) looks likely to be existed. However, the π - π stacking distance of Y258 and **14b** is longer (3.5Å), this π - π interaction could be negligible (Fig S10A). Thus, the IC₅₀ of Y258A (2.9 μ M) increased only 4.8-fold compared to that of WT (0.36 μ M). As discussed for compounds **12/13**, N125 is the residue (in helix 4) closest to C128 (Fig. S5, 3.3 Å), the addition of **14b** onto C128 will also cause the remarkable movement of N125 away from C128, which in turn significantly decrease the FBPase activity. However, when N125 was mutated to Ala, N125-S124-S123 will move close to C128, which in turn result in the increase of FBPase activity. As expected, N125A lead to the significant IC₅₀ increase (492-fold, Table S3) of **14b** compared with WT (0.36 μ M). These results further indicate that, N125-S124-S123 pathway is very important for the **14b** inhibition against FBPase, N125 is a key residue that affect the movement of

N125-S124-S123.

2.6 Inhibition of glucose output in primary rat hepatocytes.

To the best of our knowledge, FBPase is a rate-limiting enzyme in the GNG pathway, which converts carbon substrates to glucose, and is a main factor of endogenous glucose production[14, 73]. Furthermore, primary rat hepatocytes were used to explore the effect of title compounds on glucose production under physiological conditions.

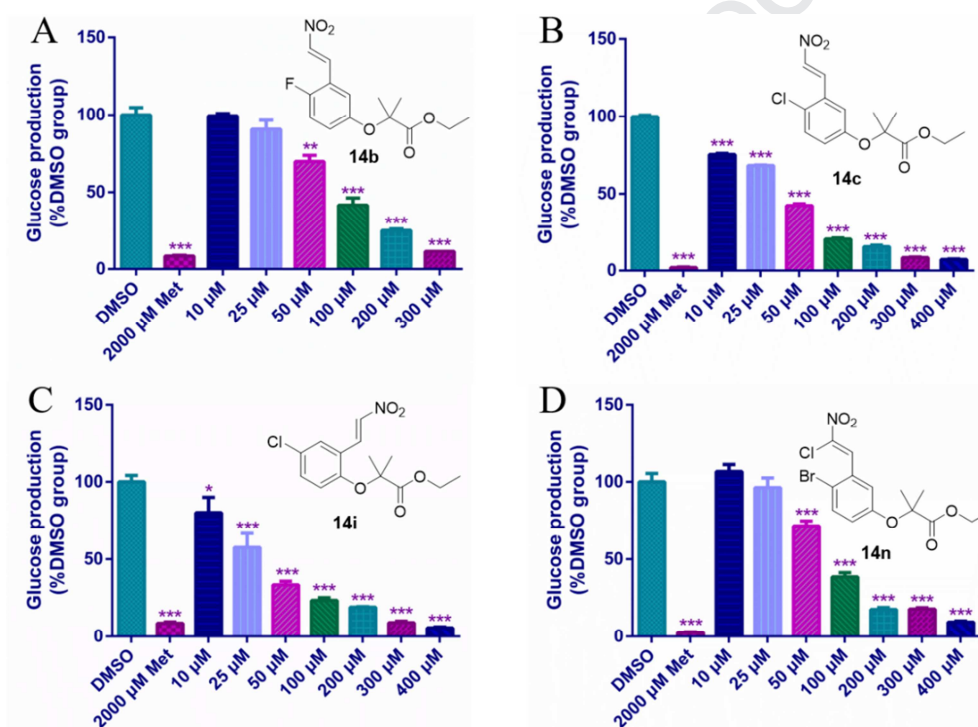


Fig. 6. Effects of Clofibrate and synthesized compounds on glucose production in primary rat hepatocytes in physical condition. **14b**(A), **14c**(B), **14i**(C), **14n**(D). * $P < 0.05$, ** $P < 0.01$, *** $P < 0.001$ vs DMSO. Data shown are means \pm SEM of four independent experiments. Metformin (Met)

As shown in Fig. 6A, B, C, D, representative compounds **14b**, **14c**, **14i** and **14n** resulted in dose-dependent inhibition of glucose production in primary rat hepatocytes.

Both **14c** (Fig. 6B) and **14i** (Fig. 6C) begin to inhibit glucose production at 10 μM , with a significant difference of $P < 0.05$ and $P < 0.01$ compared to the DMSO group. Maximal inhibition of glucose production ($\approx 90\%$) was achieved with 400 μM title compounds, and a significant difference ($P < 0.001$) was observed compared to the DMSO group. These results suggest that title compounds actually affect glucose production of the GNG pathway and that -Cl at the R_3 position is beneficial for pharmaceutical effects under physiological conditions.

In fact, the FBPase or GNG pathway is overexpressed in T2D patients[1, 2], thus, the effects of title compounds on the GNG pathway under pathological conditions were further tested (Fig. 7). It has been reported[74] that cyclic AMP (cAMP) and dexamethasone (Dex) can enhance hepatic GNG levels, therefore, this strategy was used as model for evaluation of the pharmaceutical effects. Primary rat hepatocytes were treated with 1 μM dexamethasone and 200 μM cAMP for 3 h [74, 75]. As shown in Fig. 7 vehicle, glucose production via GNG (vehicle) dramatically increased 5.8-fold compared to the DMSO group after these treatments. Consistent with the results obtained under physical conditions, the glucose lowering that occurs under pathological conditions could be observed with 1 μM **14c** (Fig. 7B) and **14i** (Fig. 7C), with a significant difference ($P < 0.001$) vs vehicle. In addition, title compounds (**14b**, **14c**, **14i**, **14n**) also caused dose-dependent (10~100 μM) inhibition of glucose production under pathological conditions ($P < 0.001$ vs vehicle). Maximal glucose lowering under pathological conditions ($\approx 95\%$) was achieved at 100 μM **14b**. In conclusion, these title compounds also exhibit potential hypoglycemic effects under

pathological conditions, even more so than under physiological conditions.

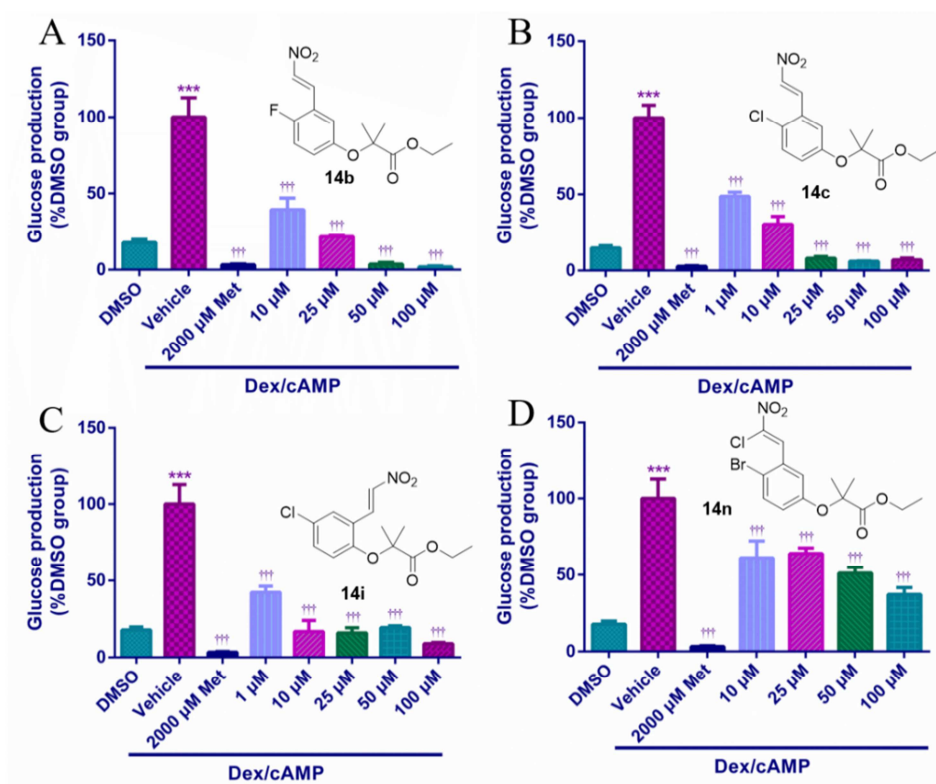


Fig. 7. Effects of title compounds (**14b**, **14c**, **14i** and **14n**) on glucose production in primary rat hepatocytes in pathology condition causing by 1 μ M dexamethasone (Dex) and 200 μ M cyclic AMP (cAMP). **14b** (A), **14c** (B), **14i** (C), **14n** (D). *** $P < 0.001$ versus DMSO. † $P < 0.05$, †† $P < 0.01$, ††† $P < 0.001$ vs vehicle. Data shown are means \pm SEM of four independent experiments.

2.7 Reducing lipid accumulation in primary rat hepatocytes.

It has been reported that high glucose and insulin levels can induce hyperglycemia and insulin resistance[76]. In particular, the title compounds were derived by combining the nitrostyrene fragment and anti-dyslipidemic functional fragments, thus, it is possible for title compounds to exhibit anti-dyslipidemic effects. Thus, this method was also used out to establish a model of lipid accumulation to

evaluate the pharmaceutical effect[77]. High concentrations of glucose (25 mM) and insulin (500 nM) were used to treat primary rat hepatocytes for 24 h resulting in lipid accumulation.

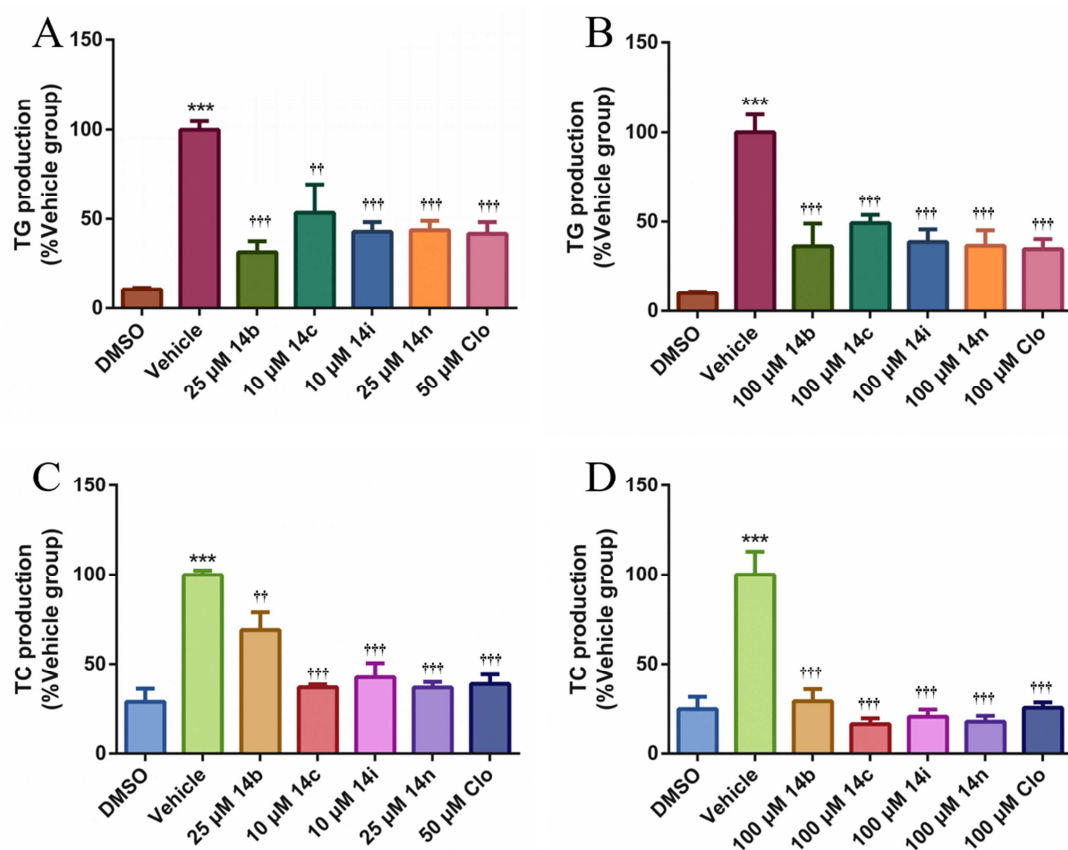


Fig. 8. Effects of title compound on lipid accumulation of TG (A, B) and TC (C, D) in primary rat hepatocytes by 25 mM high glucose and 500 nM insulin, Clo (Clofibrate). *** $P < 0.001$ vs DMSO. †† $P < 0.01$, ††† $P < 0.001$ vs vehicle. Data shown are means \pm SEM of four independent experiments.

As shown in Fig. 8, the TG and TC quality in the vehicle group increased sharply compared with that in the DMSO group, suggesting that this treatment actually led to lipid accumulation. Both **14c** and **14i** begin to show a lipid-lowering (TG and TC) effects at 25 μ M, while the minimum lipid-lowering concentration of **14b** and **14n** is 10 μ M (Fig. 8A, C). **14c** and **14i** exhibit stronger lipid-lowering effects than **14b** and

14n and, also, potentially, Clo (50 μM), as illustrated in Fig. 8A, C. Upon increasing the concentration of these compounds to 100 μM , inhibitions of TG production increased slightly (Fig. 8B), but TC production decreased markedly (Fig. 8D). Therefore, these title compounds can dose-dependently inhibit TC production, and exhibits anti-dyslipidemic activity.

2.8 Evaluation of cytotoxicity and acute toxicity.

To the best of our knowledge, a protein assay is the general experiment for the measurement of toxic substances cytotoxicity[78]. For the control of these compounds cytotoxicity, the glucose, triglyceride and total cholesterol content were normalized to the cellular protein concentration (cell viability) of primary rat hepatocytes (Fig. S11, Fig. S12, Fig. S13) as described in previous documents.[78, 79] The protein concentration of each group has been determined by using Bicinchoninic Acid (BCA) method.[79] As shown in Fig. S11, Fig. S12 and Fig. S13, most of title compounds exhibit no cytotoxicity except for **14n** in pathology condition (Fig. S14D).

In addition, Sulforhodamine B (SRB) cytotoxicity assay of primary rat hepatocytes in physical condition was further performed[80]. As shown in Fig. 9, cell viability exceeded 80% even if the concentration of compounds **14b**, **14c**, **14i** or **14n** reached 300 μM . These results further suggest that title compounds pharmaceutical effect were independent of their influences on the cell viability. Combining positive results of the protein concentration (Fig. S11, S12, S13) and SRB assay (Fig. 9), we could conclude that the hypoglycemic and hypolipidemic effects are predominantly due to the inhibition of title compounds.

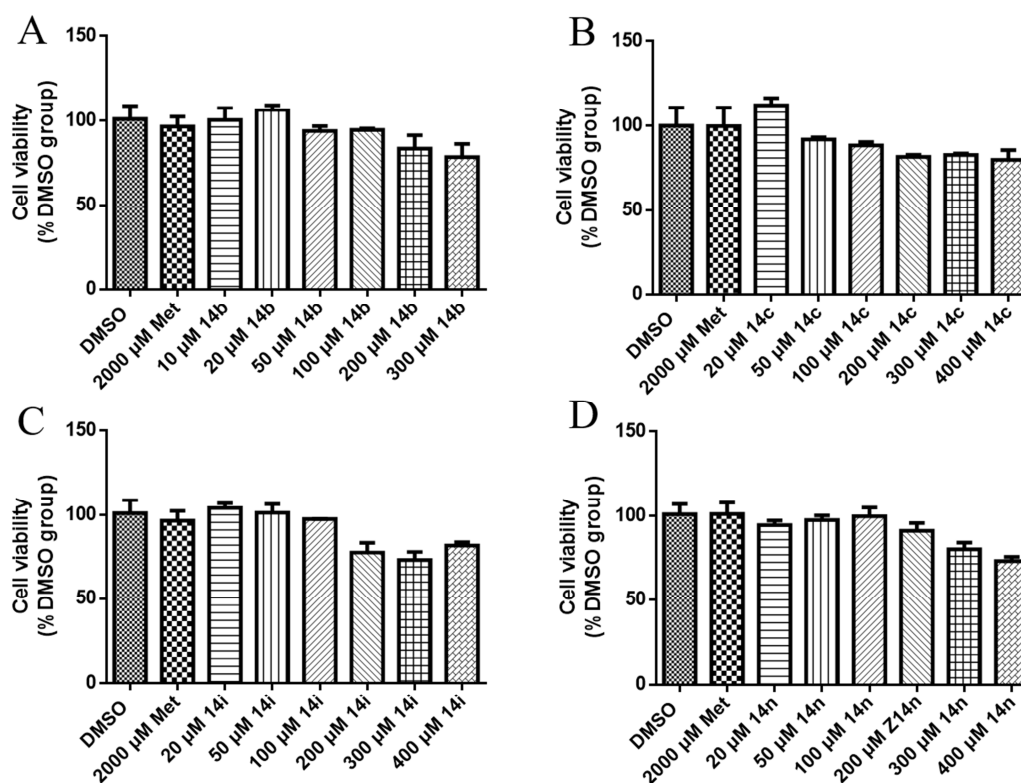


Fig. 9. The cell viability (Sulforhodamine B cytotoxicity assay, SRB) of primary rat hepatocytes in physical condition after treated by title compounds. The cell viability of **14b**(A), **14c**(B), **14i**(C), **14n**(D). Data shown are means \pm SEM of four independent experiments

Furthermore, acute toxicity of **14b** in the mice was evaluated. Sixteen 8-week-old male C57BL/6 mice were randomly divided into two groups to receive 0 (vehicle), 600 mg/kg of **14b** oral on first day. All treated animals represented no mortality, significant weight loss or allergic action and were as well health as the control animals for 14 days, indicating that **14b** has no acute toxicity at a dose of 600 mg/kg of oral (Fig. S14). These results also indicate to some extent that compounds **14b**, **14c**, **14i** and **14n** exhibit better target selectivity in primary hepatocyte.

3. Conclusion

We first discovered a novel cryptic cysteine allosteric site (C128) in FBPase, several nitrostyrene derivatives exhibiting potent FBPase inhibition ($IC_{50}=0.32 \mu\text{M}$). The N125-S124-S123 pathway was most likely involved in the allosteric regulation between C128 and active site of FBPase. However, the MS analysis revealed that these nitrostyrenes might bind with more than one cysteine besides C128 in FBPase. To improve pocket selectivity, a series of novel compounds were redesigned rationally by attaching a drug moiety with anti-dyslipidemic function to a nitrostyrene by integrating the FBCVS protocol and machine-learning-based synthetic complexity evaluation. As expected, the MS results validated the proportion of title compounds (**14b**, **14c**, **14i** or **14n**) that bind to C128 site in FBPase was higher than that of **12/13**. In addition, these title compounds not only exhibited dose-dependent (10~100 μM) inhibition of glucose production under pathological conditions ($P < 0.001$ vs vehicle) and pathological conditions but also might dose-dependently reduce the production of TG and TC. These positive results provide further evidence that molecular targeting of the C128 site of FBPase can have anti-T2D effects. This strategy could provide an alternative general approach for improvement of the selectivity and dual-functionalization of covalent drugs in the future.

4. Experimental section

4.1 Chemicals.

The following chemicals were commercially obtained and used without further purification: compounds **1~9**, 99% pure, Sigma-Aldrich; compound **10** 98% pure, Cayman; Nitrostyrene compounds **11~13**, and compounds **14a-14n** were synthesized

as described in Scheme S1, S2 and S3, and characterized as described in the Supplementary Methods, and the characteristics and purity matched those of published standards.

4.2 FBPase inhibition assays and mutagenesis.

Positive transformants containing FBPase genes were transformed into *E.coli* BL21 (DE3) for protein expression. Cloning, expression, and purification were performed as described in our previous work[81]. The final purified proteins were validated by SDS-PAGE and preserved in 50% (v/v) glycerol at -20 °C.

FBPase activity was measured by the method of malachite green[82]. 30 µL reaction solution contained 300 nM Hu-FBPase, 50 mM Tris-HCl (pH 7.4), 0.8 mM Mg²⁺, 0.4 mM FBP and 0.5 µL DMSO. All compounds were dissolved by DMSO. The reaction time is 5 min, and the reaction temperature is 37 °C. Then, the reaction was stopped by 15 µL 1M perchloric acid. The released phosphate was further to form a colored complex that was detected spectrophotometrically at 620 nm. Thus, the reaction solution was incubated with 450 µL malachite green solution (0.035% malachite green, 0.35% polyvinyl alcohol) at 25 °C for 30 min and the enzymatic activity was monitored at 620 nm. The half maximal inhibitory concentration (IC₅₀) values or kinetic constants were identified using logistic equations (nonlinear analysis) or Hill kinetic equations in the Origin 7.5 program package. All of the FBPase mutants were also expressed, purified and analyzed.

4.3 Fragment-based covalent virtual screen

Fragment-based *de novo* design is a well-developed technique for lead discovery and optimization.[83, 84] Recently, some computational fragment-based *de novo* design methods for non-covalent drugs have been implemented by using commercial or academic software, such as LUDI,[85] EA-inventor,[86] SPROUT,[87] BUILDER,[88] PROLIGANDS,[89] LigBuilder[90] and LEA3D,[91] and many protocols have been successfully used for the discovery of highly potent inhibitors.[92-94] However, fragment-based virtual screens are rare. Herein, a new FBCVS protocol (Fig. S8) was developed by integrating covalent docking (Autodock[56]), non-covalent fragment-based dock (Surflex-dock@Sybyl[95]) and multi-scoring functions (PM7@MOPAC[96]), the synthetic complexity score (SCscore) developed by Green et al.[66]). First, the covalent warhead moiety (nitrostyrene fragment) was docked covalently into the C128 site on FBPase by Autodock v4.2[56], and the conformer with highest score was chosen as the conformer of the warhead. Subsequently, the functional fragments (Fig. S9), built from commercial anti-dyslipidemic drugs[67-72], were docked into the C128 active site of FBPase by Surflex-Dock@Sybylx1.3[95]. The resulting conformations were connected to generate new non-covalent moieties, and the top 3 conformers were chosen for each compound. In the linking procedure, the linker fragment (Fig. S15) was inserted based on the distance between the two resulting conformations. The N-N, N-O and O-O bonds were excluded due to the instability of these bonds.

Then, new non-covalent moieties (~125) were docked again into the active site by Surflex-Dock@Sybylx1.3 to generate approximately 370 non-covalent

conformations. Furthermore, these non-covalent conformations were connected with the covalent warhead to generate approximately 2327 covalent molecules.

After that, synthetic difficulty for these 2327 covalent molecules was predicted by SCScore[66], obtained by deep learning from the Reaxys reaction database. According to the document of Green et al.,[66] SCScore greater than 3 indicates high difficulty of synthesis, therefore, molecules with SCScore > 3 were excluded and approximately 70 compounds remained. Finally, the optimization and binding-energy evaluations for these 70 compounds were performed at a semi-empirical quantum chemical computation level (PM7@MOPAC[96]), as illustrated in Fig. S16.

4.4 Glucose production assay

To measure the pharmaceutical effects of title compounds under physiological conditions, primary hepatocytes were separated from C57BLKS rats as previously reported[97]. Then the cells were incubated overnight with DMEM (Dulbecco's modified Eagle's medium) containing 10% fetal bovine serum (FBS). The medium was then replaced with fresh medium, and the rat primary hepatocytes cells were incubated with title compounds for 3 h. After this procedure, the medium was replaced with glucose-free DMEM containing 2 mM sodium pyruvate, 20 mM sodium lactate and the title compounds. After 3 h of incubation, the medium was subjected to glucose quantification using a glucose assay kit (BiosinoBio-Technology and Science Inc.)

To identify the effects of title compounds on gluconeogenesis under pathological conditions, and cAMP resulting upregulation of rat primary hepatocyte

gluconeogenesis were used in a mouse pathological model of T2D. After growth in DMEM containing 10% FBS overnight, the rat primary hepatocytes were pretreated with 200 μ M cAMP and 1 μ M Dex for 3 h. Finally, the cells were washed with glucose-free DMEM and cultured in glucose-free DMEM containing 2 mM sodium pyruvate, 20 mM sodium lactate and title compounds. Then, the glucose formed by gluconeogenesis was quantified as described above. The glucose, triglyceride and total cholesterol content were normalized to the cellular protein concentration[97]. The protein concentration of each group has been determined by using Bicinchoninic Acid (BCA) method [79].

4.5 Lipid accumulation assay

After treating with DMEM overnight, the rat primary hepatocytes pretreated with title compounds existed in 25 mM high glucose and 500 nM insulin for 24 h. Then, TG and TC were analyzed using two assay kits (BiosinoBio-Technology and Science Inc.).

4.6 Mass spectrometry

Liquid chromatography–mass spectrometry (LC–MS) analyses were performed in positive-ion mode with an Agilent 6550 quadrupole-time-of-flight (QTOF) mass spectrometer (Santa Clara, CA) coupled with an Agilent 1260 high-performance liquid chromatograph (HPLC; Santa Clara, CA). The native protein was also detected as a control (wild-type FBPase: 38009 Da).

4.7 Sulforhodamine B cytotoxicity assay

Rat hepatocytes were treated title compounds for 6h. Then (Sulforhodamine B

cytotoxicity assay) SRB assay was performed for detection title compounds cytotoxicity as previously described[80].

4.8 Molecular dynamics

The active crystal structure of human FBPase has not been reported. However, the active crystal structure of porcine FBPase has been reported (1EYI) and it has 90% homology with human. Thus, human active state FBPase structure was built by homology modeling according to porcine FBPase crystal structure (1EYI). FBP conformation and coordinate reference the F6P (1EYI). Then, compound **12** was covalently docked into this homologous modular structure.

The Cys-**12**, FBP was optimized by Gaussian 09[98] at the ω b97xd/6-31g(d) level, and then the atomic partial charges were obtained by fitting the electrostatic potentials using the BCC fitting technique in Amber16 [99, 100]. The generations of the partial charges and the force field parameters for CYS-**12** and FBP were accomplished using the antechamber program in AMBER16[101].

In the molecular mechanics (MM) optimizations and MD simulations, AMBER10 force field[102], and gaff force field [103] were used, respectively. The simulation was performed at pH 7.0, and the titratable residues, including lysine, arginine, aspartic acid, and glutamic acid, were typically charged, the histidine residues were protonated at the epsilon position. The whole system was immersed with TIP3P water molecules[104] in a truncated octahedron box of 10 Å from any solute atoms. The system was neutralized with the counterions of Na⁺. First the protein was restrained, and solvent molecules and ions were relaxed (2000 cycles of steepest descent and 2000 cycles of conjugate gradient minimizations). Second, the

protein backbone was restrained, and the side chains were minimized (2500 cycles of steepest descent and 2500 cycles of conjugate gradient minimizations). Finally, the whole system was minimized without any restraint (2500 cycles of steepest descent and 2500 cycles of conjugate gradient minimizations). the MD simulations of 100 ns were performed at 310K. SHAKE[105] was used to constrain bonds involving hydrogen atoms, and the time step was 2.0 fs. The nonbonded cutoff was set to 10 Å. the long-range electrostatics were calculated by the particle mesh Ewald (PME) algorithm[106].

4.9 Dilution experiment

The FBPase (300 nM) was incubated with 10× the IC₅₀ concentration of compounds **12** and **13** for complete inhibition. Then, the mixture was diluted 20 folds yielding an inhibitor concentration of 0.5× the IC₅₀, then the enzyme was activated by adding the FBP (0.4 mM) and Mg²⁺ (0.8 mM). All the wells for the enzyme reaction were diluted from the above mixture to ensure that the components were the same. The enzyme reactions were stopped by 1M perchloric acid at different times (30 min, 60 min, 90 min, 120 min, 150 min, 180 min). Then, malachite green was added to above wells to detect FBPase activity.

Author information

Corresponding author

To whom correspondence should be addressed. Phone: +86-27-67862022. Fax: +86-27-67862022. E-mails: renyl@mail.ccnu.edu.cn; jianwan@mail.ccnu.edu.cn

Author contributions

All authors contributed to the writing of the manuscript and have approved the final version of the manuscript. *These authors contributed equally. (Match statement to author names with a symbol)

Notes

The authors declare no competing financial interest.

Acknowledgements

This work was supported by the Natural Science Foundation of China (Nos. 21877046, 21873035, 21572077 and 21472061), the Program for the PCSIRT (No. IRT0953), and the self-determined research funds of CCNU from the colleges' basic research and operation of MOE (Nos. CCNU19TS011, CCNU18TS010, 2018YBZZ019, CCNU16A02041 and CCNU14A05006), Natural Science Research Project of Anhui Higher Education Institution (Key Project, KJ2018A0040), the support from the Program of Introducing Talents of Discipline to Universities of China (111 Program, B17019) is also appreciated.

Abbreviations

FBPase: fructose-1,6-bisphosphatase; FBP: fructose-1,6-biphosphate; F6P: fructose-6-biphosphate; IC₅₀: half maximal inhibitory concentration; T2D: Type 2 diabetes; SAR: structure–activity relationship; GNG: gluconeogenesis; AMP: adenosine monophosphate; DMEM: Dulbecco's modified Eagle's medium; FBDD: fragment-based drug discovery; TG: triglycerides; TC: total cholesterol; GPCRs:

G-protein-coupled receptors; cAMP: Cyclic Adenosine monophosphate; ; Dex: dexamethasone; FBCVS: fragment-based covalent virtual screening; NSCLCs: non-small-cell lung carcinomas; β ME: β -mercaptoethanol;

References

- [1] S. Andrikopoulos, J. Proietto, The biochemical basis of increased hepatic glucose production in a mouse model of type 2 (non-insulin-dependent) diabetes mellitus, *Diabetologia*, 38 (1995) 1389-1396.
- [2] M. Kebede, J. Favalaro, J.E. Gunton, D.R. Laybutt, M. Shaw, N. Wong, B.C. Fam, K. Aston-Mourney, C. Rantza, A. Zulli, J. Proietto, S. Andrikopoulos, Fructose-1,6-Bisphosphatase Overexpression in Pancreatic β -Cells Results in Reduced Insulin Secretion: A New Mechanism for Fat-Induced Impairment of β -Cell Function, *Diabetes*, 57 (2008) 1887-1895.
- [3] Z. Wei, E. Yoshihara, N. He, N. Hah, W. Fan, A.F.M. Pinto, T. Huddy, Y. Wang, B. Ross, G. Estepa, Y. Dai, N. Ding, M.H. Sherman, S. Fang, X. Zhao, C. Liddle, A.R. Atkins, R.T. Yu, M. Downes, R.M. Evans, Vitamin D Switches BAF Complexes to Protect β Cells, *Cell*, (2018).
- [4] L.K.J. Stadler, I.S. Farooqi, A New Drug Target for Type 2 Diabetes, *Cell*, 170 (2017) 12-14.
- [5] A.K. Rines, K. Sharabi, C.D.J. Tavares, P. Puigserver, Targeting hepatic glucose metabolism in the treatment of type 2 diabetes, *Nat. Rev. Drug Discov.*, 15 (2016) 786-804.
- [6] S.E. Kahn, M.E. Cooper, S. Del Prato, Pathophysiology and treatment of type 2 diabetes: perspectives on the past, present, and future, *The Lancet*, 383 (2014) 1068-1083.
- [7] N. Kerru, A. Singh-Pillay, P. Awolade, P. Singh, Current anti-diabetic agents and their molecular targets: A review, *Eur. J. Med. Chem.*, 152 (2018) 436-488.
- [8] D.E. Moller, New drug targets for type 2 diabetes and the metabolic syndrome, *Nature*, 414 (2001) 821-827.
- [9] A. Wagman, J. Nuss, Current Therapies and Emerging Targets for the Treatment of Diabetes, *Curr. Pharm. Des.*, 7 (2001) 417-450.
- [10] M.D. Erion, Q. Dang, M.R. Reddy, S.R. Kasibhatla, J. Huang, W.N. Lipscomb, P.D. van Poelje, Structure-guided design of AMP mimics that inhibit fructose-1,6-bisphosphatase with high affinity and specificity, *J. Am. Chem. Soc.*, 129 (2007) 15480-15490.
- [11] M.D. Erion, P.D. van Poelje, Q. Dang, S.R. Kasibhatla, S.C. Potter, M.R. Reddy, K.R. Reddy, T. Jiang, W.N. Lipscomb, MB06322 (CS-917): A potent and selective inhibitor of fructose 1,6-bisphosphatase for controlling gluconeogenesis in type 2 diabetes, *Proc. Natl. Acad. Sci. U S A*, 102 (2005) 7970-7975.
- [12] P.D. van Poelje, Q. Dang, M.D. Erion, Fructose-1,6-bisphosphatase as a therapeutic target for type 2 diabetes, *Drug Discov. Today*, 4 (2007) 103-109.
- [13] R. Kaur, L. Dahiya, M. Kumar, Fructose-1,6-bisphosphatase inhibitors: A new valid approach for management of type 2 diabetes mellitus, *Eur. J. Med. Chem.*, 141 (2017) 473-505.
- [14] P.D. van Poelje, S.C. Potter, V.C. Chandramouli, B.R. Landau, Q. Dang, M.D. Erion, Inhibition of fructose 1,6-bisphosphatase reduces excessive endogenous glucose production and attenuates hyperglycemia in Zucker diabetic fatty rats, *Diabetes*, 55 (2006) 1747-1754.
- [15] Q. Dang, P.D. Van Poelje, M.D. Erion, The Discovery and Development of MB07803, a Second-Generation Fructose-1,6-bisphosphatase Inhibitor with Improved Pharmacokinetic Properties,

- as a Potential Treatment of Type 2 Diabetes, in: R.M. Jones (Ed.), *New Therapeutic Strategies for Type 2 Diabetes: Small Molecule Approaches*, Royal Society of Chemistry, London, (2012) 306-323.
- [16] E.S. Kim, S. Dhillon, Ibrutinib: a review of its use in patients with mantle cell lymphoma or chronic lymphocytic leukaemia, *Drugs*, 75 (2015) 769-776.
- [17] S.E. Dalton, L. Dittus, D.A. Thomas, M.A. Convery, J. Nunes, J.T. Bush, J.P. Evans, T. Werner, M. Bantscheff, J.A. Murphy, S. Campos, Selectively Targeting the Kinome-Conserved Lysine of PI3Kdelta as a General Approach to Covalent Kinase Inhibition, *J. Am. Chem. Soc.*, 140 (2018) 932-939.
- [18] S.M. Haag, M.F. Gulen, L. Reymond, A. Gibelin, L. Abrami, A. Decout, M. Heymann, F.G. van der Goot, G. Turcatti, R. Behrendt, A. Ablasser, Targeting STING with covalent small-molecule inhibitors, *Nature*, 559 (2018) 269-273.
- [19] S. De Cesco, J. Kurian, C. Dufresne, A.K. Mittermaier, N. Moitessier, Covalent inhibitors design and discovery, *Eur. J. Med. Chem.*, 138 (2017) 96-114.
- [20] R. Lonsdale, R.A. Ward, Structure-based design of targeted covalent inhibitors, *Chem. Soc. Rev.*, 47 (2018) 3816-3830.
- [21] J. Plescia, S. De Cesco, M.B. Patrascu, J. Kurian, J. Di Trani, C. Dufresne, A.S. Wahba, N. Janmamode, A.K. Mittermaier, N. Moitessier, Integrated Synthetic, Biophysical, and Computational Investigations of Covalent Inhibitors of Prolyl Oligopeptidase and Fibroblast Activation Protein alpha, *J. Med. Chem.*, 62 (2019) 7874-7884.
- [22] T.A. Baillie, Targeted Covalent Inhibitors for Drug Design, *Angew. Chem. Int. Ed. Engl.*, 55 (2016) 13408-13421.
- [23] K. K., Hallenbecka, David M. Turnera, Adam R. Rensloa, M.R. Arkina, Targeting Non-Catalytic Cysteine Residues Through Structure-Guided Drug Discovery, *Curr. Top. Med. Chem.*, 17 (2017) 4-15.
- [24] T. Barf, A. Kaptein, Irreversible Protein Kinase Inhibitors: Balancing the Benefits and Risks, *J. Med. Chem.*, 55 (2012) 6243-6262.
- [25] S.M. Marino, V.N. Gladyshev, Analysis and functional prediction of reactive cysteine residues, *J. Biol. Chem.*, 287 (2012) 4419-4425.
- [26] J. Singh, R.C. Petter, T.A. Baillie, A. Whitty, The resurgence of covalent drugs, *Nat. Rev. Drug Discov.*, 10 (2011) 307-317.
- [27] T. Barf, A. Kaptein, Irreversible protein kinase inhibitors: balancing the benefits and risks, *J. Med. Chem.*, 55 (2012) 6243-6262.
- [28] D.M. Rosenbaum, C. Zhang, J.A. Lyons, R. Holl, D. Aragao, D.H. Arlow, S.G. Rasmussen, H.J. Choi, B.T. Devree, R.K. Sunahara, P.S. Chae, S.H. Gellman, R.O. Dror, D.E. Shaw, W.I. Weis, M. Caffrey, P. Gmeiner, B.K. Kobilka, Structure and function of an irreversible agonist-beta(2) adrenoceptor complex, *Nature*, 469 (2011) 236-240.
- [29] M. Hagel, D. Niu, T. St Martin, M.P. Sheets, L. Qiao, H. Bernard, R.M. Karp, Z. Zhu, M.T. Labenski, P. Chaturvedi, M. Nacht, W.F. Westlin, R.C. Petter, J. Singh, Selective irreversible inhibition of a protease by targeting a noncatalytic cysteine, *Nat. Chem. Biol.*, 7 (2011) 22-24.
- [30] M.R. Janes, J. Zhang, L.S. Li, R. Hansen, U. Peters, X. Guo, Y. Chen, A. Babbar, S.J. Firdaus, L. Darjania, J. Feng, J.H. Chen, S. Li, S. Li, Y.O. Long, C. Thach, Y. Liu, A. Zarieh, T. Ely, J.M. Kucharski, L.V. Kessler, T. Wu, K. Yu, Y. Wang, Y. Yao, X. Deng, P.P. Zarrinkar, D. Brehmer, D. Dhanak, M.V. Lorenzi, D. Hu-Lowe, M.P. Patricelli, P. Ren, Y. Liu, Targeting KRAS Mutant Cancers with a Covalent G12C-Specific Inhibitor, *Cell*, 172 (2018) 578-589 e517.
- [31] G. Craven, D. Affron, C. Allen, S. Matthies, J. Greener, R. Morgan, E. Tate, A. Armstrong, D.J. Mann, High-Throughput Kinetic Analysis for Target-Directed Covalent Ligand Discovery, *Angew.*

Chem. Int. Ed. Engl., (2018).

- [32] D. Beglov, D.R. Hall, A.E. Wakefield, L. Luo, K.N. Allen, D. Kozakov, A. Whitty, S. Vajda, Exploring the structural origins of cryptic sites on proteins, *Proc. Natl. Acad. Sci. U S A*, 115 (2018) E3416-E3425.
- [33] D.L. Bourdet, K. Lee, D.R. Thakker, Photoaffinity labeling of the anionic sites in Caco-2 cells mediating saturable transport of hydrophilic cations ranitidine and famotidine, *J. Med. Chem.*, 47 (2004) 2935-2938.
- [34] N.D. Yeomans, Z. Tulassay, L. Juhasz, I. Racz, J.M. Howard, C.J. van Rensburg, A.J. Swannell, C.J. Hawkey, A comparison of omeprazole with ranitidine for ulcers associated with nonsteroidal antiinflammatory drugs. Acid Suppression Trial: Ranitidine versus Omeprazole for NSAID-associated Ulcer Treatment (ASTRONAUT) Study Group, *N. Engl. J. Med.*, 338 (1998) 719-726.
- [35] R.M. Lago, P.P. Singh, R.W. Nesto, Diabetes and hypertension, *Nat. Clin. Pract. Endocrinol. Metab.*, 3 (2007) 667.
- [36] P. Gaede, P. Vedel, N. Larsen, G.V. Jensen, H.H. Parving, O. Pedersen, Multifactorial intervention and cardiovascular disease in patients with type 2 diabetes, *N. Engl. J. Med.*, 348 (2003) 383-393.
- [37] G.I. Shulman, Ectopic fat in insulin resistance, dyslipidemia, and cardiometabolic disease, *N. Engl. J. Med.*, 371 (2014) 1131-1141.
- [38] D.L. Bhatt, K.A. Fox, W. Hacke, P.B. Berger, H.R. Black, W.E. Boden, P. Cacoub, E.A. Cohen, M.A. Creager, J.D. Easton, M.D. Flather, S.M. Haffner, C.W. Hamm, G.J. Hankey, S.C. Johnston, K.H. Mak, J.L. Mas, G. Montalescot, T.A. Pearson, P.G. Steg, S.R. Steinhubl, M.A. Weber, D.M. Brennan, L. Fabry-Ribaudo, J. Booth, E.J. Topol, C. Investigators, Clopidogrel and aspirin versus aspirin alone for the prevention of atherothrombotic events, *N. Engl. J. Med.*, 354 (2006) 1706-1717.
- [39] Y. Bansal, O. Silakari, Multifunctional compounds: Smart molecules for multifactorial diseases, *Eur. J. Med. Chem.*, 76 (2014) 31-42.
- [40] D.A. Erlanson, S.W. Fesik, R.E. Hubbard, W. Jahnke, H. Jhoti, Twenty years on: the impact of fragments on drug discovery, *Nat. Rev. Drug Discov.*, 15 (2016) 605.
- [41] J.A. Hardy, J. Lam, J.T. Nguyen, T. O'Brien, J.A. Wells, Discovery of an allosteric site in the caspases, *Proc. Natl. Acad. Sci. U S A*, 101 (2004) 12461-12466.
- [42] Jonathan M. Ostrem, Ulf Peters, Martin L. Sos, James A. Wells, K.M. Shokat, K-Ras(G12C) inhibitors allosterically control GTP affinity and effector interactions, *Nature*, 503 (2013) 548-551.
- [43] G.-J. M, Z. Y, v.P. PD, L. JY, H. S, K. J, E. JT, E. MD, The allosteric site of human liver fructose-1,6-bisphosphatase. Analysis of six AMP site mutants based on the crystal structure, *J. Biol. Chem.*, 269 (1994) 27732-27738.
- [44] J.-Y. Choe, H.J. Fromm, R.B. Honzatko, Crystal Structures of Fructose 1,6-Bisphosphatase: Mechanism of Catalysis and Allosteric Inhibition Revealed in Product Complexes, *Biochemistry*, 39 (2000) 8565-8574.
- [45] P.A. Jackson, J.C. Widen, D.A. Harki, K.M. Brummond, Covalent Modifiers: A Chemical Perspective on the Reactivity of alpha,beta-Unsaturated Carbonyls with Thiols via Hetero-Michael Addition Reactions, *J. Med. Chem.*, (2016).
- [46] P. Ábrányi-Balogh, L. Petri, T. Imre, P. Szijj, A. Scarpino, M. Hrast, A. Mitrović, U.P. Fonovič, K. Németh, H. Barreteau, D.I. Roper, K. Horváti, G.G. Ferenczy, J. Kos, J. Ilaš, S. Gobec, G.M. Keserű, A road map for prioritizing warheads for cysteine targeting covalent inhibitors, *Eur. J. Med. Chem.*, 160 (2018) 94-107.
- [47] T.K. Rudolph, B.A. Freeman, Transduction of redox signaling by electrophile-protein reactions,

Sci. Signal., 2 (2009) re7.

[48] F. Schopfer, C. Cipollina, B. Freeman, Formation and Signaling Actions of Electrophilic Lipids, *Chem. Rev.*, 111 (2011) 5997-6021.

[49] B. Carlos, F.J. Schopfer, P.R.S. Baker, D. Rosario, L.M.S. Baker, H. Yingying, C.A. Carlos, B.P. Branchaud, B.A. Freeman, Reversible post-translational modification of proteins by nitrated fatty acids in vivo, *J. Biol. Chem.*, 281 (2006) 20450-20463.

[50] R. Bompreszi, Dimethyl fumarate in the treatment of relapsing-remitting multiple sclerosis: an overview, *Ther. Adv. Neurol. Disord.*, 8 (2015) 20-30.

[51] Z. Zeng, Z. Sun, M. Huang, W. Zhang, J. Liu, L. Chen, F. Chen, Y. Zhou, J. Lin, F. Huang, L. Xu, Z. Zhuang, S. Guo, G. Alitongbieke, G. Xie, Y. Xu, B. Lin, X. Cao, Y. Su, X.K. Zhang, H. Zhou, Nitrostyrene Derivatives Act as RXR α Ligands to Inhibit TNF α Activation of NF- κ B, *Cancer Res.*, 75 (2015) 2049-2060.

[52] Y. He, S. Varadarajan, R. Munoz-Planillo, A. Burberry, Y. Nakamura, G. Nunez, 3,4-methylenedioxy-beta-nitrostyrene inhibits NLRP3 inflammasome activation by blocking assembly of the inflammasome, *J. Biol. Chem.*, 289 (2014) 1142-1150.

[53] A. Latorre, T. Schirmeister, J. Kesselring, S. Jung, P. Johe, U.A. Hellmich, A. Heilos, B. Engels, R.L. Krauth-Siegel, N. Dirdjaja, L. Bou-Iserte, S. Rodriguez, F.V. Gonzalez, Dipeptidyl Nitroalkenes as Potent Reversible Inhibitors of Cysteine Proteases Rhodasein and Cruzain, *ACS Med. Chem. Lett.*, 7 (2016) 1073-1076.

[54] A.G. Baldwin, D. Brough, S. Freeman, Inhibiting the Inflammasome: A Chemical Perspective, *J. Med. Chem.*, 59 (2016) 1691-1710.

[55] I.M. Serafimova, M.A. Pufall, S. Krishnan, K. Duda, M.S. Cohen, R.L. Maglathlin, J.M. McFarland, R.M. Miller, M. Frodin, J. Taunton, Reversible targeting of noncatalytic cysteines with chemically tuned electrophiles, *Nat. Chem. Biol.*, 8 (2012) 471-476.

[56] G.M. Morris, H. Ruth, L. William, M.F. Sanner, R.K. Belew, D.S. Goodsell, A.J. Olson, AutoDock4 and AutoDockTools4: Automated docking with selective receptor flexibility, *J. Comput. Chem.*, 30 (2010) 2785-2791.

[57] J. Park, D. Pei, trans-Beta-nitrostyrene derivatives as slow-binding inhibitors of protein tyrosine phosphatases, *Biochemistry*, 43 (2004) 15014-15021.

[58] S. Parvez, M.J.C. Long, J.R. Poganik, Y. Aye, Redox Signaling by Reactive Electrophiles and Oxidants, *Chem. Rev.*, 118 (2018) 8798-8888.

[59] Y.Q. Sun, M. Chen, J. Liu, X. Lv, J.F. Li, W. Guo, Nitroolefin-based coumarin as a colorimetric and fluorescent dual probe for biothiols, *Chem. Commun.*, 47 (2011) 11029-11031.

[60] A. Latorre, T. Schirmeister, J. Kesselring, S. Jung, P. Johe, U.A. Hellmich, A. Heilos, B. Engels, R.L. Krauth-Siegel, N. Dirdjaja, L. Bou-Iserte, S. Rodriguez, F.V. Gonzalez, Dipeptidyl Nitroalkenes as Potent Reversible Inhibitors of Cysteine Proteases Rhodasein and Cruzain, *ACS Med. Chem. Lett.*, 7 (2016) 1073-1076.

[61] C. Batthyany, F.J. Schopfer, P.R. Baker, R. Duran, L.M. Baker, Y. Huang, C. Cervenansky, B.P. Branchaud, B.A. Freeman, Reversible post-translational modification of proteins by nitrated fatty acids in vivo, *J. Biol. Chem.*, 281 (2006) 20450-20463.

[62] J.M. Ostrem, U. Peters, M.L. Sos, J.A. Wells, K.M. Shokat, K-Ras(G12C) inhibitors allosterically control GTP affinity and effector interactions, *Nature*, 503 (2013) 548.

[63] S.G. Kathman, Z. Xu, A.V. Statsyuk, A fragment-based method to discover irreversible covalent inhibitors of cysteine proteases, *J. Med. Chem.*, 57 (2014) 4969-4974.

- [64] C.N. Johnson, D.A. Erlanson, C.W. Murray, D.C. Rees, Fragment-to-Lead Medicinal Chemistry Publications in 2015, *J. Med. Chem.*, 60 (2017) 89-99.
- [65] G.M. Keseru, D.A. Erlanson, G.G. Ferenczy, M.M. Hann, C.W. Murray, S.D. Pickett, Design Principles for Fragment Libraries: Maximizing the Value of Learnings from Pharma Fragment-Based Drug Discovery (FBDD) Programs for Use in Academia, *J. Med. Chem.*, 59 (2016) 8189-8206.
- [66] C.W. Coley, L. Rogers, W.H. Green, K.F. Jensen, SCScore: Synthetic Complexity Learned from a Reaction Corpus, *J. Chem. Inf. Model.*, 58 (2018) 252-261.
- [67] R.W. Sarver, E. Bills, G. Bolton, L.D. Bratton, N.L. Caspers, J.B. Dunbar, M.S. Harris, R.H. Hutchings, R.M. Kennedy, S.D. Larsen, A. Pavlovsky, J.A. Pfefferkorn, G. Bainbridge, Thermodynamic and Structure Guided Design of Statin Based Inhibitors of 3-Hydroxy-3-Methylglutaryl Coenzyme A Reductase, *J. Med. Chem.*, 51 (2008) 3804-3813.
- [68] C.P. Cannon, M.A. Blazing, R.P. Giugliano, A. McCagg, J.A. White, P. Theroux, H. Darius, B.S. Lewis, T.O. Ophuis, J.W. Jukema, G.M. De Ferrari, W. Ruzyllo, P. De Lucca, K. Im, E.A. Bohula, C. Reist, S.D. Wiviott, A.M. Tershakovec, T.A. Musliner, E. Braunwald, R.M. Califf, Ezetimibe Added to Statin Therapy after Acute Coronary Syndromes, *N. Engl. J. Med.*, 372 (2015) 2387-2397.
- [69] C. Pirat, A. Farce, N. Lebegue, N. Renault, C. Furman, R. Millet, S. Yous, S. Specca, P. Berthelot, P. Desreumaux, P. Chavatte, Targeting peroxisome proliferator-activated receptors (PPARs): development of modulators, *J. Med. Chem.*, 55 (2012) 4027-4061.
- [70] T. Kumari, U. Issar, R. Kakkar, Docking modes of BB-3497 into the PDF active site--a comparison of the pure MM and QM/MM based docking strategies, *Curr. Comput. Aided Drug Des.*, 10 (2014) 315-326.
- [71] U. Julius, Niacin as antidyslipidemic drug, *Can. J. Physiol. Pharmacol.*, 93 (2015) 1043-1054.
- [72] R.L. Pollex, T.R. Joy, R.A. Hegele, Emerging antidyslipidemic drugs, *Expert Opin. Emerg. Drugs*, 13 (2008) 363-381.
- [73] D. Rothman, I. Magnusson, L. Katz, R. Shulman, G. Shulman, Quantitation of hepatic glycogenolysis and gluconeogenesis in fasting humans with ¹³C NMR, *Science*, 254 (1991) 573-576.
- [74] J.C. Yoon, P. Puigserver, G. Chen, J. Donovan, Z. Wu, J. Rhee, G. Adelmant, J. Stafford, C.R. Kahn, D.K. Granner, C.B. Newgard, B.M. Spiegelman, Control of hepatic gluconeogenesis through the transcriptional coactivator PGC-1, *Nature*, 413 (2001) 131-138.
- [75] M. Matsumoto, A. Pocai, L. Rossetti, R.A. Depinho, D. Accili, Impaired regulation of hepatic glucose production in mice lacking the forkhead transcription factor Foxo1 in liver, *Cell Metab.*, 6 (2007) 208-216.
- [76] Y. Li, S. Xu, M.M. Mihaylova, B. Zheng, X. Hou, B. Jiang, O. Park, Z. Luo, E. Lefai, J.Y. Shyy, B. Gao, M. Wierzbicki, T.J. Verbeuren, R.J. Shaw, R.A. Cohen, M. Zang, AMPK phosphorylates and inhibits SREBP activity to attenuate hepatic steatosis and atherosclerosis in diet-induced insulin-resistant mice, *Cell Metab.*, 13 (2011) 376-388.
- [77] T. Zheng, X. Yang, D. Wu, S. Xing, F. Bian, W. Li, J. Chi, X. Bai, G. Wu, X. Chen, Y. Zhang, S. Jin, Salidroside ameliorates insulin resistance through activation of a mitochondria-associated AMPK/PI3K/Akt/GSK3beta pathway, *Br. J. Pharmacol.*, 172 (2015) 3284-3301.
- [78] G. Fotakis, J.A. Timbrell, In vitro cytotoxicity assays: comparison of LDH, neutral red, MTT and protein assay in hepatoma cell lines following exposure to cadmium chloride, *Toxicol. Lett.*, 160 (2006) 171-177.
- [79] A.M. Hall, V. Croy, ., T. Chan, ., D. Ruff, ., T. Kuczek, ., C. Chang, . Bicinchoninic acid protein assay in the determination of adriamycin cytotoxicity modulated by the MDR glycoprotein, *J. Nat.*

- Prod., 59 (1996) 35-40.
- [80] V. Vichai, K. Kirtikara, Sulforhodamine B colorimetric assay for cytotoxicity screening, *Nat. Protoc.*, 1 (2006) 1112.
- [81] X. Han, Y. Huang, R. Zhang, S. Xiao, S. Zhu, N. Qin, Z. Hong, L. Wei, J. Feng, Y. Ren, L. Feng, J. Wan, New insight into the binding modes of TNP-AMP to human liver fructose-1,6-bisphosphatase, *Spectrochim. Acta. A Mol. Biomol. Spectrosc.*, 165 (2016) 155-160.
- [82] T.W. Von Geldern, C. Lai, R.J. Gum, M. Daly, C. Sun, E.H. Fry, C. Abad-Zapatero, Benzoxazole benzenesulfonamides are novel allosteric inhibitors of fructose-1,6-bisphosphatase with a distinct binding mode, *Bioorg. Med. Chem. Lett.*, 16 (2006) 1811-1815.
- [83] D.A. Erlanson, S.W. Fesik, R.E. Hubbard, W. Jahnke, H. Jhoti, Twenty years on: the impact of fragments on drug discovery, *Nat. Rev. Drug Discov.*, 15 (2016) 605-619.
- [84] N. Fuller, L. Spadola, S. Cowen, J. Patel, H. Schonherr, Q. Cao, A. McKenzie, F. Edfeldt, A. Rabow, R. Goodnow, An improved model for fragment-based lead generation at AstraZeneca, *Drug Discov. Today*, 21 (2016) 1272-1283.
- [85] H.-J. Böhm, The computer program LUDI: A new method for the de novo design of enzyme inhibitors, *J. Comput. Aided Mol. Des.*, 6 (1992) 61-78.
- [86] Q. Liu, B. Masek, K. Smith, J. Smith, Tagged fragment method for evolutionary structure-based de novo lead generation and optimization, *J. Med. Chem.*, 50 (2007) 5392-5402.
- [87] V.J. Gillet, W. Newell, P. Mata, G. Myatt, S. Sike, Z. Zsoldos, A.P. Johnson, SPROUT: recent developments in the de novo design of molecules, *J. Chem. Inf. Comput. Sci.*, 34 (1994) 207-217.
- [88] D.C. Roe, I.D. Kuntz, BUILDER v.2: Improving the chemistry of a de novo design strategy, *J. Comput. Aided Mol. Des.*, 9 (1995) 269-282.
- [89] B. Waszkowycz, D.E. Clark, D. Frenkel, J. Li, C.W. Murray, B. Robson, D.R. Westhead, PRO_LIGAND: an approach to de novo molecular design. 2. Design of novel molecules from molecular field analysis (MFA) models and pharmacophores, *J. Med. Chem.*, 37 (1994) 3994-4002.
- [90] R. Wang, Y. Gao, L. Lai, LigBuilder: A Multi-Purpose Program for Structure-Based Drug Design, *Mol. Model. Annual*, 6 (2000) 498-516.
- [91] D. Douguet, H. Munierlehmman, G. Labesse, S. Pochet, LEA3D: a computer-aided ligand design for structure-based drug design, *J. Med. Chem.*, 48 (2005) 2457-2468.
- [92] G.-F. Hao, F. Wang, H. Li, X.-L. Zhu, W.-C. Yang, L.-S. Huang, J.-W. Wu, E.A. Berry, G.-F. Yang, Computational Discovery of Picomolar Qo Site Inhibitors of Cytochrome bc1 Complex, *J. Am. Chem. Soc.*, 134 (2012) 11168-11176.
- [93] F. Svensson, A. Bender, D. Bailey, Fragment-Based Drug Discovery of Phosphodiesterase Inhibitors, *J. Med. Chem.*, 61 (2018) 1415-1424.
- [94] Y. Li, Z. Zhao, Z. Liu, M. Su, R. Wang, AutoT&T v.2: An Efficient and Versatile Tool for Lead Structure Generation and Optimization, *J. Chem. Inf. Model.*, 56 (2016) 435-453.
- [95] A. Jain, Surflex-Dock 2.1: Robust performance from ligand energetic modeling, ring flexibility, and knowledge-based search, *Journal of Computer-Aided Molecular Design*, 21 (2007) 281-306.
- [96] J.J.P. Stewart, MOPAC2016, Stewart Computational Chemistry, Colorado Springs, CO, USA, [HTTP://OpenMOPAC.net](http://OpenMOPAC.net), (2016).
- [97] Q.F. Collins, H.-Y. Liu, J. Pi, Z. Liu, M.J. Quon, W. Cao, Epigallocatechin-3-gallate (EGCG), A Green Tea Polyphenol, Suppresses Hepatic Gluconeogenesis through 5'-AMP-activated Protein Kinase, *J. Biol. Chem.*, 282 (2007) 30143-30149.

- [98] M.J. Frisch, G.W. Trucks, H.B. Schlegel, G.E. Scuseria, M.A. Robb, J.R. Cheeseman, J.A. Montgomery, Jr., T.K. Vreven, K. N. ; , J.C. Burant, J.M. Millam, S.S. Iyengar, J.B. Tomasi, V., B.C. Mennucci, M., G.R. Scalmani, N., G.A. Petersson, H. Nakatsuji, M.E. Hada, M., K. Toyota, R. Fukuda, J. Hasegawa, M. Ishida, T. Nakajima, Y. Honda, O. Kitao, H. Nakai, M. Klene, X. Li, J.E. Knox, H.P. Hratchian, J.B. Cross, V. Bakken, C. Adamo, J. Jaramillo, R. Gomperts, R.E. Stratmann, O. Yazyev, A.J. Austin, R.P. Cammi, C., J.W. Ochterski, P.Y. Ayala, K. Morokuma, G.A. Voth, P. Salvador, J.J. Dannenberg, V.G. Zakrzewski, S. Dapprich, A.D. Daniels, M.C. Strain, O. Farkas, D.K. Malick, A.D. Rabuck, K. Raghavachari, J.B. Foresman, J.V. Ortiz, Q. Cui, A.G. Baboul, S. Clifford, J. Cioslowski, B.B. Stefanov, G. Liu, A. Liashenko, P. Piskorz, I. Komaromi, R.L. Martin, D.J. Fox, T. Keith, M.A. Al-Laham, C.Y. Peng, A. Nanayakkara, M. Challacombe, P.M.W. Gill, B. Johnson, W. Chen, M.W. Wong, C. Gonzalez, J.A. Pople, Gaussian 03, revision C. 02; Gaussian, Inc.: Wallingford, CT, 2004.
- [99] A. Jakalian, B.L. Bush, D.B. Jack, C.I. Bayly, Fast, efficient generation of high-quality atomic charges. AM1-BCC model: I. Method, *J. Comput. Chem.*, 21 (2000) 132-146.
- [100] A. Jakalian, D.B. Jack, C.I. Bayly, Fast, efficient generation of high-quality atomic charges. AM1-BCC model: II. Parameterization and validation, *J. Comput. Chem.*, 23 (2002) 1623-1641.
- [101] J. Wang, W. Wang, P.A. Kollman, D.A. Case, Automatic atom type and bond type perception in molecular mechanical calculations, *J. Mol. Graph. Model.*, 25 (2006) 247-260.
- [102] Y. Duan, C. Wu, S. Chowdhury, M.C. Lee, G. Xiong, W. Zhang, R. Yang, P. Cieplak, R. Luo, T. Lee, J. Caldwell, J. Wang, P. Kollman, A point-charge force field for molecular mechanics simulations of proteins based on condensed-phase quantum mechanical calculations, *J. Comput. Chem.*, 24 (2003) 1999-2012.
- [103] J. Wang, R.M. Wolf, J.W. Caldwell, P.A. Kollman, D.A. Case, Development and testing of a general amber force field, *J. Comput. Chem.*, 25 (2004) 1157-1174.
- [104] W.L. Jorgensen, J. Chandrasekhar, J.D. Madura, R.W. Impey, M.L. Klein, Comparison of simple potential functions for simulating liquid water, *The Journal of Chemical Physics*, 79 (1983) 926-935.
- [105] J.-P. Ryckaert, G. Ciccotti, H.J.C. Berendsen, Numerical integration of the cartesian equations of motion of a system with constraints: molecular dynamics of n-alkanes, *J. Comput. Phys.*, 23 (1977) 327-341.
- [106] T. Darden, D. York, L. Pedersen, Particle mesh Ewald: An $N \cdot \log(N)$ method for Ewald sums in large systems, *J. Comput. Phys.*, 98 (1993) 10089-10092.